doi:10.1016/j.jmb.2006.02.016 J. Mol. Biol. (2006) 358, 347–354

JMB

Available online at www.sciencedirect.com

SCIENCE DIRECT®

ELSEVIER

COMMUNICATION

Crystal Structure of the TCR Co-receptor CD8αα in Complex with Monoclonal Antibody YTS 105.18 Fab Fragment at 2.88 Å Resolution

D. A. Shore[1,2], L. Teyton[3], R. A. Dwek[2], P. M. Rudd[2] and I. A. Wilson[1,4]*

[1]*Department of Molecular Biology, The Scripps Research Institute, La Jolla, CA 92037 USA*

[2]*Department of Biochemistry Oxford Glycobiology Institute University of Oxford, South Parks Road, Oxford OX1 3QU, UK*

[3]*Department of Immunology The Scripps Research Institute La Jolla, CA 92037, USA*

[4]*Skaggs Institute for Chemical Biology, The Scripps Research Institute, La Jolla CA 92037, USA*

**Corresponding author*

The CD8 glycoprotein functions as an essential element in the control of T-cell selection, maturation and the TCR-mediated response to peptide antigen. CD8 is expressed as both heterodimeric CD8αβ and homodimeric CD8αα isoforms, which have distinct physiological roles and exhibit tissue-specific expression patterns. CD8αα has previously been crystallized in complex with class I pMHC and, more recently, with the mouse class Ib thymic leukemia antigen (TL). Here, we present the crystal structure of a soluble form of mouse CD8αα in complex with rat monoclonal antibody YTS 105.18 Fab fragment at 2.88 Å resolution. YTS 105.18, which is commonly used in the blockade of $CD8^+$ T-cell activation in response to peptide antigen, is specific for mouse CD8α. The YTS 105.18 Fab is one of only five rat IgG Fab structures to have been reported to date. Analysis of the YTS 105.18 Fab epitope on CD8α reveals that this antibody blocks CD8 activity by hydrogen bonding to residues that are critical for interaction with both class I pMHC and TL. Structural comparison of the liganded and unliganded forms of soluble CD8αα indicates that the mouse CD8αα immunoglobulin-domain dimer does not undergo significant structural alteration upon interaction either with class I pMHC or TL.

Keywords: CD8; X-ray structure; antibody structure; T-cell; immune system

The CD8 glycoprotein comprises alpha (α) and beta (β) subunits, and is expressed at the leucocyte cell surface as a disulphide-linked dimer of either αα or αβ. Although CD8α and CD8β share less than 20% sequence identity, and are under the influence of separate promoter elements, they have a similar topology.[1,2] Each subunit comprises an immunoglobulin super-family (IgSF) variable-type domain, a highly *O*-glycosylated Ser/Thr/Pro-rich extended stalk region consisting of 30–51 residues, a single-pass transmembrane region and a short intracellular domain.[3] The IgSF domains of each subunit combine to form the binding site with which CD8 interacts with class I ligands on the surface of antigen presenting cells.[3] *N*-Glycosylation of the CD8 IgSF domains is highly variable; in humans, only a single site on CD8β is *N*-glycosylated whereas, in rat, the α and β subunits have one and three *N*-glycosylation sites, respectively, and in mouse, the reverse is found where the α and β subunits have three and one *N*-glycosylation sites, respectively. *O*-Glycosylation of the extended stalk region of each subunit is important in the selection, maturation and activation of $CD8^+$ T-cells.[4,5] The cytoplasmic domain of CD8α is associated[6] with the tyrosine kinase $p56^{LcK}$, and the intracellular region of CD8β facilitates the interaction of this subunit with the intracellular components of the TCR/CD3 complex within membrane rafts on the T-cell surface.[7]

The predominant isoform on circulating $CD8^+$ leucocytes is CD8αβ, which binds to the non-polymorphic region of the class I major histocompatibility complex (MHC) during antigen recognition by the αβT-cell receptor (TCR) to function as a co-stimulatory factor for the TCR-mediated response to class I MHC-bound peptide antigen (pMHC) (reviewed by van de Merwe & Davis[8]). CD8αα is found mainly on intra-epithelial

Abbreviations used: IgSF, immunoglobulin super-family; MHC, major histocompatibility complex; IEL, intra-epithelial leucocytes; TL, thymic leukaemia antigen; CDR, complementarity determining region.

E-mail address of the corresponding author: wilson@scripps.edu

leucocytes (IEL), natural killer cells (NK) and γδT-cells, but has also been identified on both $CD8^+$ and $CD4^+$ circulatory αβT-cells.[9]

The physiological role of CD8αα is less well defined than that of CD8αβ; CD8αα is expressed at lower levels on conventional $CD8^+$ T-cells than the αβ isoform, and is 100-fold less effective than CD8αβ as a co-receptor for TCR-mediated T-cell activation.[10,11] A high level of CD8αα on the surface of IELs in the gut appears to be of functional significance to these cells that play a regulatory, rather than cytotoxic, role (reviewed by Gangadharan & Cheroutre[12]). Furthermore, expression of CD8αα has also been associated with the initiation and maintenance of $CD8^+$ T-cell memory.[13,14]

In contrast to CD8αβ, CD8αα preferentially binds to the mouse class Ib thymic leukemia antigen (TL). Tetramers of TL bind with a higher affinity to cells expressing the homotypic CD8αα than to those expressing CD8αβ, and soluble TL has a greater affinity for immobilized CD8αα (K_D=12 μM) than for immobilized CD8αβ (K_D=>90 μM).[15] The interaction of CD8αα with TL is antigen-independent and is thought to perform a regulatory role in T-cell homeostasis that is distinct from the function of CD8αβ interaction with class I pMHC.[16] CD8αα has also been identified in association with a 180 kDa epithelial cell surface glycoprotein (gp180) in man, although the biological significance of this interaction has yet to be determined.[17]

Overall structure of the CD8αα/YTS 105.18 complex

The crystal structure of the mouse CD8αα IgSF domain dimer has previously been reported in complex with class I pMHC H-$2K^b$ to 2.8 Å resolution,[18] as well as in complex with mouse class Ib TL to 2.1 Å resolution.[19] Here, we report the crystal structure of a mouse CD8αα IgSF domain dimer in complex with rat $IgG2_a$ YTS 105.18 antibody Fab fragment at 2.88 Å resolution. This complex defines the structure of the mouse CD8αα dimer in the absence of class I pMHC or TL, and identifies the epitope for YTS 105.18 on CD8α. The crystallographic asymmetric unit contains a single CD8αα homodimer, bound on each side by a YTS 105.18 Fab (Fab1 and Fab2), as illustrated in Figure 1(a).

The refined model contains 1081 residues of the 1102 present in the complex, as well as 12 well-defined water molecules. Residues 1–228 of the Fab heavy chain, residues 1–211 of the light chain, residues 4–123 of the CD8α1 subunit and residues 4–122 of the CD8α2 subunit are observed in the electron density maps. Stereochemical analysis shows 86.3%, 11.6% and 2.0% of the residues are within the most favored, allowed and generously allowed regions of the Ramachandran plot, respectively.[20] AlaL51 lies within the disallowed region of the Ramachandran plot, but is situated within a classic γ-turn motif that is commonly observed in antibody Fabs.[21]

The CD8α IgSF domain adopts the classical immunoglobulin V-type fold, composed of nine β-strands, which form the classic sandwich of two antiparallel β-sheets. A small region of both CD8α1 and CD8α2 (Lys69, Asn70, Ser71 and Ser72) is not included within the refined model due to disorder. Despite the presence of three potential *N*-linked carbohydrate sites on CD8αα, no interpretable electron density was observed for carbohydrates attached at either Asn42 or Asn70. The third potential *N*-glycosylation site at Asn123 is not included within the CD8α construct. The $2F_o-F_c$ electron density is well-defined for all of the V_H, V_L, C_H1 and C_L domains of the Fab except for a small region of the C_H1 domain that forms a highly flexible loop (Asp130, Thr131 and Thr132) and is commonly disordered in almost all Fab crystal structures.[21] This region of the Fab has been omitted

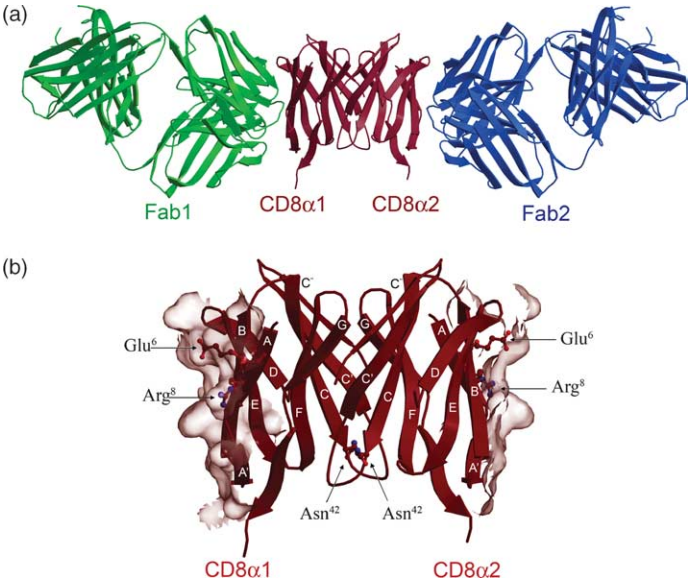

Figure 1. Mouse CD8αα complex with the YTS 105.18 Fab. (a) Ribbon diagram of the refined model of the CD8αα/YTS 105.18 Fab complex. Fab1 and Fab2 are in green and blue, respectively. The CD8α1 and CD8α2 subunits are in maroon. (b) The epitope for the YTS 105.18 Fab on the surface of the CD8αα subunit. YTS 105.18 binds the A, A′ and B strands of CD8α. The epitope molecular surface (grey) covered by YTS 105.18 is superimposed on the ribbon diagram of CD8αα. Arg8 and Glu6 of CD8α, which are involved in hydrogen bonding to class I pMHC, TL and also to YTS 105.18 Fab, are indicated. The single *N*-glycosylation site at Asn42 within the CD8 construct is also indicated.

from the model due to lack of interpretable electron density.

The YTS 105.18 Fab combining site

The YTS 105.18 Fab crystal structure is one of only five rat IgG Fab structures to have been reported so far and is the only anti-CD8 antibody Fab structure to have been described. The YTS 105.18 epitope on mouse CD8α is illustrated in Figure 1(b). The refined model has an excellent fit to electron density in the region of the CD8αα/YTS 105.18 Fab interface, which is located on the A, A′ and B strands of the CD8α IgSF domain and involves residues from all six complementarity determining region (CDR) loops of the YTS 105.18 Fab. The topology of the YTS 105.18 Fab combining site is typical of anti-protein antibodies with a concave and undulating surface.[21] The surface areas buried upon complex formation between CD8α and YTS 105.18 Fab are 771 Å^2 and 747 Å^2, respectively, and are typical of those observed for protein/antibody interactions.[21] The majority of the Fab combining site interactions are within V_H, which contributes 64% of the buried surface area.

Comparison with TL and class-I pMHC bound mouse CD8αα

The structure of the mouse CD8αα IgSF domain has been described in complex with class I pMHC H-2K^b (PDB entry 1BQH[18]) and in complex with class 1b TL (PDB entry 1NEZ[19]). Hence, the structure presented here represents the first view of mouse CD8αα in the absence of an MHC ligand. Comparison of CD8αα from our structure with those from the class I pMHC and TL complexes, after superimposition of the 224 C$^\alpha$ atoms of CD8αα reveals no significant changes in CD8αα upon binding H-2K^b or TL (Figure 2(a)), with r.m.s.d values of only 0.75 Å and 0.67 Å, respectively. Thus, there is no evidence to suggest that conformational changes or induced-fit mechanisms in the IgSF domains are involved in the functional activity of mouse CD8αα. The CDR-equivalent loop regions at the top of the CD8α IgSF domains, comprising Gly30 to Gly35 (CDR1-eqivalent), Tyr55 to Lys62 (CDR2-equivalent) and Val104 to Tyr111 (CDR3-equivalent) are involved in the interaction of CD8α with both class I pMHC and TL.[22] In our structure, the CDR-like loops of CD8αα are not involved in crystal contacts, and the average *B* values for residues within CDR1 (49 Å^2) and CDR2 (47 Å^2) are only slightly higher than those of the CD8αα IgSF dimer as a whole (42 Å^2), whereas those for CDR3 are slightly lower (36 Å^2). An alignment of the β-sheet regions of CD8αα from our structure with those from the class I pMHC and TL complex structures was carried out to assess any conformational variations in the CDR-like loop regions between unliganded and liganded forms of mouse CD8αα (Figure 2(b)). Small variations arise in the CDR1 and CDR2-equivalent loops, although the CDR3-equivalent loop regions exhibit very little variation.

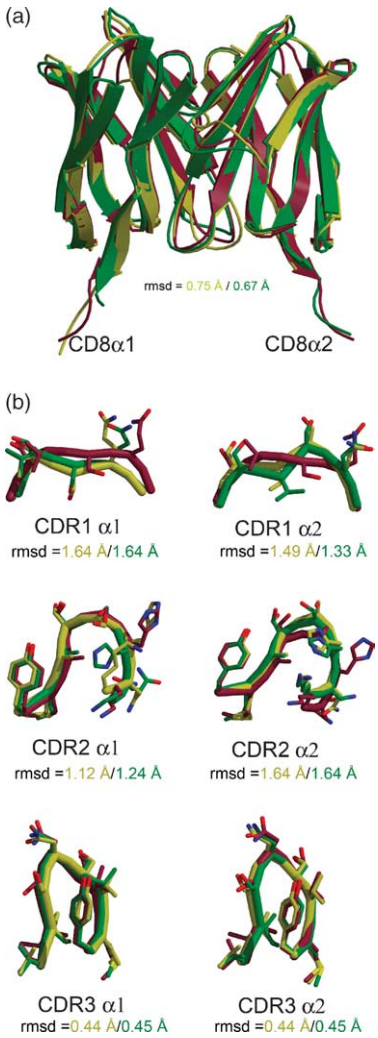

Figure 2. Comparison of Fab-bound, pMHC-bound and TL-bound CD8αα. (a) Superimposition of the Fab-bound CD8αα (maroon) with CD8αα from the complexes with TL (dark green) and class I pMHC (yellow). Superimposition was carried out using C$^\alpha$ atoms from 224 residues corresponding to the CD8αα dimers of each structure. (b) Overlay of residues within the CDR-equivalent loops of CD8αα from our structure (maroon) and those within the CDR-equivalent loops of CD8αα in the complexes with TL (dark green) and with class I pMHC (yellow). Superimposition of loop regions was carried out based on an alignment of the β-sheet regions of CD8αα from each structure and r.m.s.d. values are based on atoms in the main-chain residues of each loop.

Molecular basis of YTS 105.18 blocking activity

YTS 105.18 is a rat IgG$_{2a}$ anti-CD8α monoclonal antibody that does not deplete CD8$^+$ T-cells *in vivo* and is widely used for the blockade of CD8$^+$ T-cell activity in mice.[23] Inoculation of mice with YTS 105.18 induces tolerance to zenograft transplan-

tation[24] and reduces insulin-dependent diabetes mellitus (IDDM) in NOD mice.[25]

Comparison of the class I pMHC binding site of CD8α, as defined in the CD8αα/H-2K^b complex structure,[18] with the YTS 105.18 epitope determined here indicates that residues of CD8α that interact with the β_2M and α3 domains of class I pMHC are also involved in the interaction with YTS 105.18. The YTS 105.18/CD8αα complex structure shows hydrogen bond formation between Glu6 and Glu27 of CD8α with TyrL53 and TyrH100 of YTS, respectively (Figure 3(a)). However, the CD8αα/

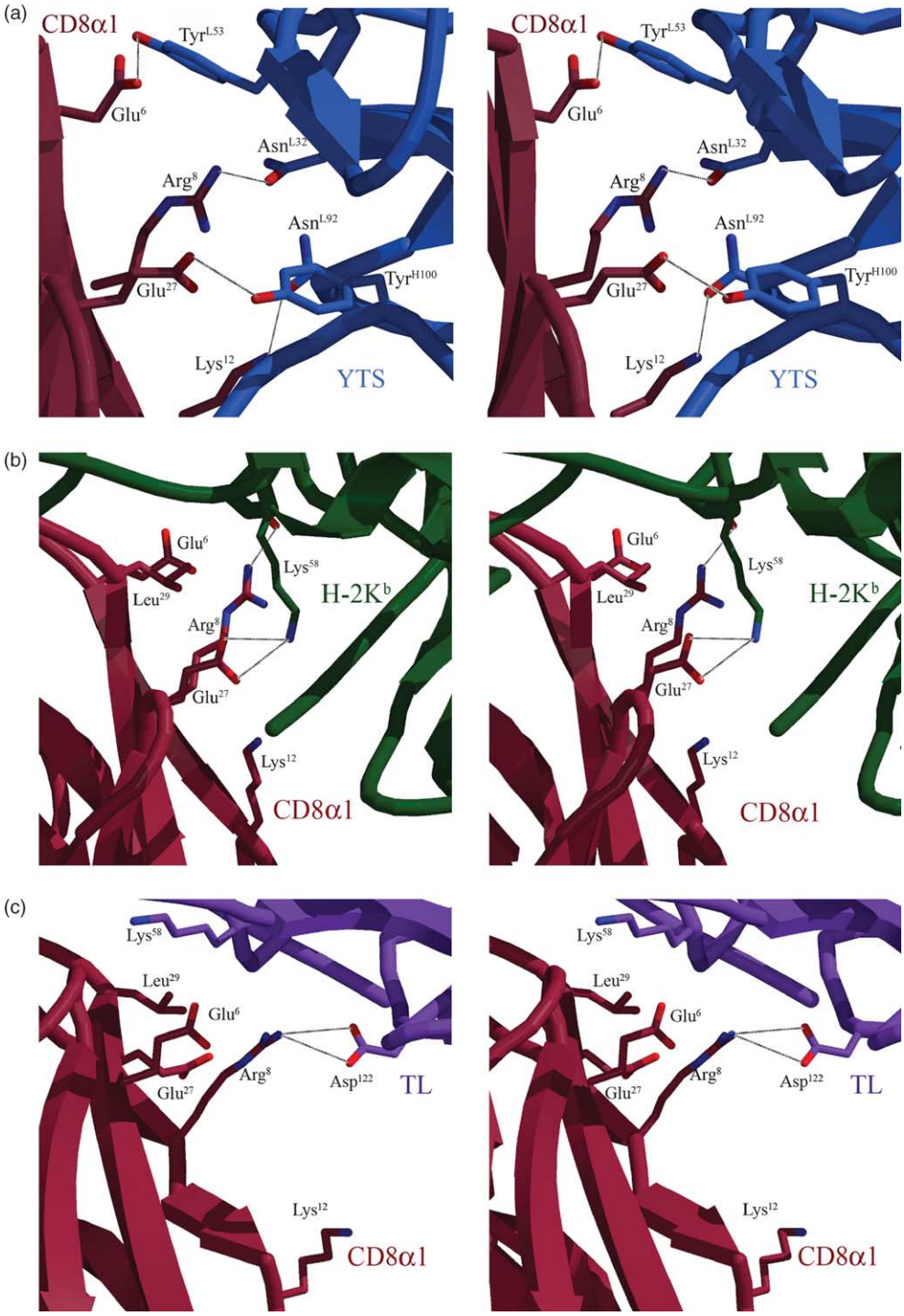

Figure 3. Comparison of CD8α interaction with YTS 105.18, H-2K^b and TL. (a) Expanded view of the interface between CD8α and YTS 105.18 Fab in stereo. The CD8αα/Fab complex is orientated as in Figure 1(a), with CD8α1 (maroon) on the left and YTS 105.18 Fab1 (blue) on the right. Hydrogen bonds are indicated by a broken line. (b) Equivalent stereo view of the interaction of CD8α1 (maroon) with class I pMHC (green), as defined in the CD8αα/H-2K^b complex structure.[18] (c) Equivalent stereo view of the interaction between CD8α1 (maroon) and TL (purple), as defined in the CD8αα/TL complex structure.[19]

class I pMHC complex structure reveals a salt-bridge between Glu6 and Arg8 of CD8αα that helps orient and stabilize the interaction between Arg8 and the main chain carbonyl of β_2M Lys58, which also hydrogen bonds to Glu27 of CD8α (Figure 3(b)). In YTS 105.18, Arg8 of CD8α hydrogen bonds to the side-chain of AsnL32 of YTS 105.18 (Figure 3(a)). Mutation of Arg8 to Ala8 in mouse CD8α was previously found to inhibit binding of soluble CD8αα to class I pMHC, suggesting that interaction between Arg8 and Lys58 of β_2M is critical.[22] Likewise, given that the interaction between CD8α and TL as defined in the CD8αα/TL complex structure[19] involves formation of a salt-bridge and hydrogen bonds between Arg8 of CD8α with Asp122 of the TL α2 domain (Figure 3(c)), it is likely that binding of CD8α with YTS 105.18 would also inhibit the interaction of CD8αα with TL.

Recent structural studies have revealed that the CD8α and CD8β subunits have a similar topology, and the CD8αβ IgSF-domain dimer is strikingly similar to that of CD8αα.[2] Furthermore, mutations of Arg4 (to Lys4) and Leu25 (to Ala25) of human CD8α have an adverse affect upon the interaction in human CD8αβ with class I pMHC.[26] It is reasonable to assume, therefore, that CD8αβ binds class I pMHC in a similar disposition to CD8αα, such that the CD8α subunit contacts the α1, α2 and β_2M domains. Superimposition of the mouse CD8αα/H-2K^b structure with the CD8αα/Fab structure in the region of the CD8αα dimer indicates that Fab binding sterically hinders interaction of CD8αα with class I pMHC and, therefore, would inhibit binding of CD8αβ to class I pMHC. A physical clash would occur either between the YTS 105.18 Fab and the α1/α2 domains of the class I pMHC (Figure 4(a)), or between the YTS 105.18 Fab and the APC membrane (Figure 4(b)), depending upon the disposition of the CD8α subunit on CD8αβ relative to class I pMHC. However, it should be noted that the connecting peptide that tethers the class I pMHC to the APC membrane is highly flexible and the orientation of class I/CD8αβ complex relative to the membrane is, therefore, dynamic and could possibly accommodate binding to CD8αβ/YTS 105.18 if CD8α occupies the "lower"

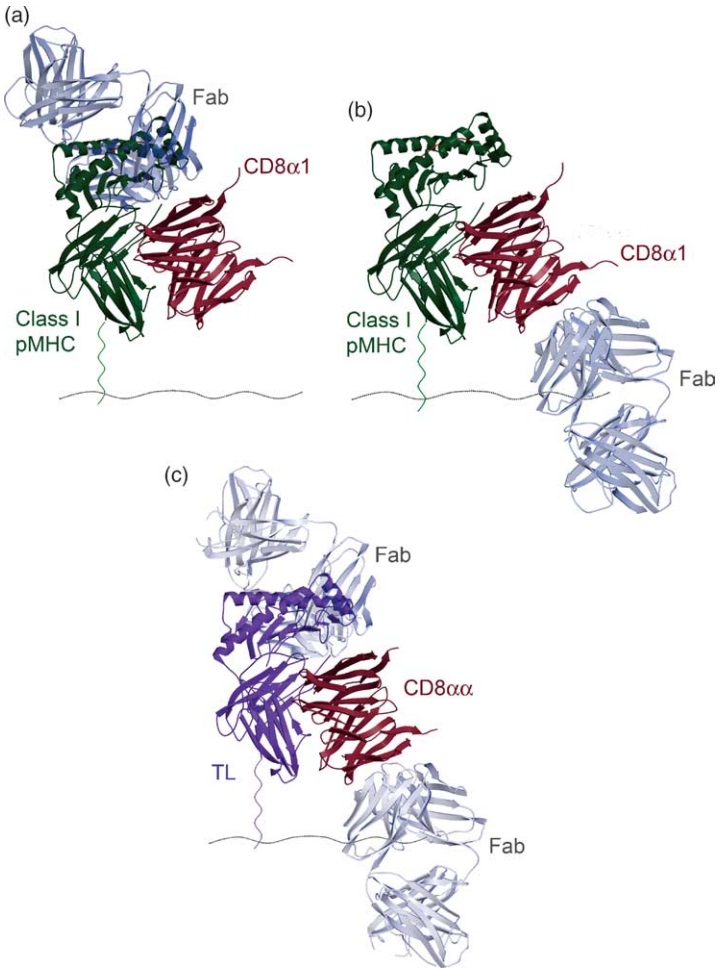

Figure 4. Mechanism of YTS 105.18 inhibition of CD8 binding to class I pMHC and TL. Superimposition of the CD8αα/YTS 105.18 Fab complex with the CD8αα/class I pMHC complex over the C$^\alpha$ atoms in 224 residues of CD8αα provides two alternative models for the inhibition of CD8αβ binding to class I pMHC, dependent on the disposition of CD8α relative to CD8β in the CD8αβ/pMHC complex. The class I pMHC is depicted in green, CD8αα is in maroon and the YTS 105.18 Fab is in grey. A peptide loaded within the antigen-presenting groove of class I pMHC is represented in red, and the flexible connecting peptide is modeled at the carboxyl terminus of the class I α3 domain. The APC membrane is represented at the membrane-proximal end of the class I pMHC (broken line). (a) If CD8α occupies the "upper" position of the class I pMHC binding site, CD8αβ/pMHC complex formation is inhibited by YTS 105.18, by clash between YTS 105.18 Fab and the α1 and α2 domains of class I pMHC. (b) If CD8α occupies the alternative, "lower" position, inhibition of CD8αβ/pMHC complex formation would occur by a clash between YTS 105.18 and the APC membrane when CD8αβ attempts to dock with class I pMHC. (c) Overlay of the CD8αα/TL complex structure[18] with the CD8αα/YTS 105.18 Fab complex structure to illustrate two possible mechanisms of inhibition of CD8αα/TL complex formation by YTS 105.18. The models have been aligned through C$^\alpha$ atoms of CD8αα from each structure. TL is depicted in purple, CD8αα in maroon and the YTS 105.18 Fab is in grey. The flexible connecting peptide that tethers TL to the APC membrane is modeled at the carboxyl terminus of TL. The APC membrane is represented at the membrane-proximal end of TL (broken line).

(α2) half of the binding site. However, CD8αβ likely binds class I pMHC such that the CD8α subunit occupies the "upper" (α1) position, but this determination must now await a CD8αβ/class I complex crystal structure.

Given that blockade of $CD8^+$ T-cell activity by YTS 105.18 is brought about by prevention of a close association between CD8αβ/YTS 105.18 and class I pMHC at the T-cell/antigen presenting cell junction, it is likely that YTS 105.18 would also inhibit interaction between CD8αα and TL at the surface of IEL and may, therefore, have an effect upon IEL proliferation, cytokine production and cell killing (Figure 4(c)).[15]

Protein expression and purification

The IgSF domain of mouse CD8α, comprising residues 1–123 of the mature protein, coupled to a C-terminal cleavable leucine-zipper and hexa-histidine purification tag (see Supplementary Data), was cloned into the *p*RHma3 expression vector (Invitrogen) and recombinant soluble CD8α was produced in the *Drosophila melanogaster* expression system. *D. melanogaster* cells recombinant for soluble mouse CD8α were cultured using Insect Express serum-free medium (Gibco) in rotating roller bottles at 28 °C. Recombinant CD8αα protein was isolated from cell-free medium by affinity chromatography using beaded Ni NTA (Qiagen) and purified to homogeneity by size-exclusion gel filtration (Superdex 75 26/60, Amersham Pharmacia Biotech) to yield 0.5 mg protein/l of tissue culture supernatant. Removal of the carboxyl-terminal leucine zipper and hexa-histidine tag was achieved by cleavage with thrombin protease to yield a 38 kDa dimer (sCD8αα).

Partial deglycosylation of recombinant glycoproteins has previously been carried out to facilitate protein crystallization and to improve the diffraction quality of crystals, by enhancing the homogeneity of attached *N*-linked carbohydrates.[27] It was determined by HPLC analysis that *N*-glycans attached to *s*CD8αα consisted of high mannose and truncated core-fucosylated structures (data not shown) resulting from the limited *N*-glycosylation capabilities of *D. melanogaster* cells.[28] Hence, removal of terminal α-1,2, α-1,3 and α-1,6-linked mannose residues attached to Asn42 and Asn70 of sCD8αα was carried out by exposure to Jack bean α-mannosidase (Sigma Aldrich) in a solution containing 0.1 M sodium acetate, 100 mM NaCl, at pH 5.6 for 18 h at 20 °C.

The YTS 105.18 mAb bound to sCD8αα with nanomolar affinity, as determined by surface plasmon resonance analysis (data not shown). The YTS 105.18 hybridoma cell line[23] was cultured in large quantities and YTS 105.18 IgG was purified from tissue culture supernatant by affinity chromatography using beaded protein G (Sigma Aldrich). YTS 105.18 Fab was obtained by digestion with 10 ng of papain protease/mg of protein (Sigma Alrich) and subsequently purified to homogeneity by size-exclusion gel filtration (Superdex 75 26/60, Amersham Pharmacia Biotech). The amino acid sequence of the YTS 105.18 Fab was determined by RT-PCR of mRNA purified from the YTS 105.18 hybridoma cell line and subsequent nucleotide sequencing of the resulting cDNA. Formation of a complex between YTS 105.18 Fab and an equimolar amount of sCD8αα was observed as a peak of the appropriate size in size-exclusion gel filtration and usable crystals were obtained from this material.

Crystallization, data collection and refinement

YTS 105.18 Fab was incubated with an equimolar amount of CD8αα for 10 min at 37 °C and crystals of the CD8αα/YTS 105.18 complex (12.5 mg/ml) grew from a solution containing 20% (w/v) PEG 3000, 100 mM sodium acetate (pH 5.1). Crystals were flash-cooled to −180 °C by rapid immersion in liquid nitrogen, in a cryo-protectant containing the well solution plus 20% (v/v) glycerol. A native dataset was collected from a single crystal to 2.88 Å resolution at the Advanced Light Source (ALS) synchrotron at the University of California, Berkeley, CA, USA (Table 1). The CD8αα/YTS 105.18 Fab complex crystallized in orthorhombic space group $P2_12_12_1$, with unit cell dimensions $a=83.8$ Å, $b=107.8$ Å, $c=134.1$ Å. The crystallographic asymmetric unit contains two Fabs and one

Table 1. Crystallographic data and refinement

A. *Data processing*	
Resolution range (Å)	50.00–2.88 (3.00–2.88)
Unique reflections	26,797 (2532)
Completeness (%)	99.1 (95.7)
Redundancy	4.3
R_{sym} [a] (%)	15.4 (60.9)
Average $I/\sigma(I)$	10.8 (1.8)
B.*Refinement*	
Reflections	25,403 (1609)
Reflections (test)	1346
R_{cryst} [b] (%)	22.8
R_{free} [c] (%)	27.3
Residues/protein atoms	1090/8341
Water molecules	12
Coordinate error[d] (Å)	0.35
rmsd bonds/angles (Å/deg.)	0.018/1.75
Average *B* values (Å^2)	
Fab1	41.3
Fab2	41.2
CD8αα	42.2
Water molecules	34.5
Ramachandran statistics (%)	
Most favored	86.3
Additionally allowed	11.6
Generously allowed	2.0
Disallowed	0.1

Values in parentheses refer to the highest resolution shell.

[a] $R_{sym} = 100\,\Sigma_h\,\Sigma_i\,|I_i(h) - \langle I(h)\rangle| / \Sigma_h\,I(h)$, where $I_i(h)$ is the *i*th measurement of the *h* reflection and $\langle I(h)\rangle$ is the average value of the reflection intensity.

[b] $R_{cryst} = \Sigma||F_o| - |F_c||/\Sigma|F_o|$, where F_o and F_c are the structure factor amplitudes form the data and the model, respectively.

[c] R_{free} is R_{cryst} with 5% of the test set structure factors.

[d] Values are based on maximum likelihood.

*s*CD8αα, with solvent content of 47.2% (v/v) and packing density (V_M) of 2.33 Å^3/Da.[29]

The data were phased by the molecular replacement method, using the program AMoRe.[30] The CD8α coordinates from the mouse CD8αα/TL complex structure (PDB entry 1NEZ[19]) and a mouse Fab structure (PDB entry 1ACY[31]) were used as search models. Refinement of the CD8αα/YTS 105.18 Fab complex structure was carried out using the crystallography and NMR system (CNS) program version 1.1,[32] and Refmac5,[33] as implemented in the CCP4 suite of programs.[34] Strict non-crystallographic symmetry (NCS) restraints were imposed upon the model throughout the refinement. Molecular model building was carried out using the program O.[35] Superimposition of molecules was carried out using the least-squares method, surface area calculations were carried out using the program MS[36] and Figures were created using the program MOLSCRIPT.[37]

Protein Data Bank accession code

Coordinates and structure factors have been deposited in the RCSB Protein Data Bank with RCSB accession number rcsb034228 and PDB ID code 2ARJ.

Acknowledgements

This work has been supported by NIH grants AI042266 to I.A.W and AI042267 to L.T. We thank Dr Xiaoping Dai as well as the staff at the ALS beam line 8.3.1 for data collection and Dr Xueyong Zhu for assistance with molecular replacement and calculations. This is manuscript number 17640-MB from the Scripps Research Institute.

Supplementary Data

Supplementary data associated with this article can be found, in the online version, at doi:10.1016/j.jmb.2006.02.016

References

1. Norment, A. M. & Littman, D. R. (1988). A second subunit of CD8 is expressed in human T cells. *EMBO J.* **7**, 3433–3439.
2. Chang, H. C., Tan, K., Ouyang, J., Parisini, E., Liu, J. H., Le., Y. *et al*. (2005). Structural and mutational analyses of a CD8αβ heterodimer and comparison with the CD8αα homodimer. *Immunity*, **6**, 661–671.
3. Kern, P., Hussey, R. E., Spoerl, R., Reinherz, E. L. & Chang, H. C. (1999). Expression, purification, and functional analysis of murine ectodomain fragments of CD8αα and CD8αβ dimers. *J. Biol. Chem.* **274**, 27237–27243.
4. Merry, A. H., Gilbert, R. J., Shore, D. A., Royle, L., Miroshnychenko, O., Vuong, M. *et al*. (2003). O-glycan sialylation and the structure of the stalk-like region of the T cell co-receptor CD8. *J. Biol. Chem.* **278**, 27119–27128.
5. Daniels, M. A., Devine, L., Miller, J. D., Moser, J. M., Lukacher, A. E., Altman, J. D. *et al*. (2001). CD8 binding to MHC class I molecules is influenced by T cell maturation and glycosylation. *Immunity*, **15**, 1051–1061.
6. Kim, P. W., Sun, Z. Y., Blacklow, S. C., Wagner, G. & Eck, M. J. (2003). A zinc clasp structure tethers Lck to T cell coreceptors CD4 and CD8. *Science*, **301**, 1725–1728.
7. Arcaro, A., Gregoire, C., Bakker, T. R., Baldi, L., Jordan, M., Goffin, L. *et al*. (2001). CD8β endows CD8 with efficient coreceptor function by coupling T cell receptor/CD3 to raft-associated CD8/p56(lck) complexes. *J. Expt. Med.* **194**, 1485–1495.
8. van der Merwe, P. A. & Davis, S. J. (2003). Molecular interactions mediating T cell antigen recognition. *Annu. Rev. Immunol.* **21**, 659–684.
9. Leishman, A. J., Gapin, L., Capone, M., Palmer, E., MacDonald, H. R., Kronenberg, M. & Cheroutre, H. (2002). Precursors of functional MHC class I- or class II-restricted CD8αα(+) T cells are positively selected in the thymus by agonist self-peptides. *Immunity*, **16**, 355–364.
10. Zamoyska, R. (1994). The CD8 coreceptor revisited: one chain good, two chains better. *Immunity*, **1**, 243–246.
11. Cawthon, A. G., Lu, H. & Alexander-Miller, M. A. (2001). Peptide requirement for CTL activation reflects the sensitivity to CD3 engagement: correlation with CD8αβ versus CD8αα expression. *J. Immunol.* **167**, 2577–2584.
12. Gangadharan, D. & Cheroutre, H. (2004). The CD8 isoform CD8αα is not a functional homologue of the TCR co-receptor CD8αβ. *Curr. Opin. Immunol.* **16**, 264–270.
13. Kim, S. V. & Flavell, R. A. (2004). Immunology. CD8αα and T cell memory. *Science*, ***304***, *529–530*.
14. Madakamutil, L. T., Christen, U., Lena, C. J., Wang-Zhu, Y., Attinger, A., Sundarrajan, M. et al. (2004). CD8aa-mediated survival and differentiation of CD8 memory T cell precursors. Science, **304**, 590–593.
15. Attinger, A., Devine, L., Wang-Zhu, Y., Martin, D., Wang, J. H., Reinherz, E. L. et al. (2005). Molecular basis for the high affinity interaction between the thymic leukemia antigen and the CD8αα molecule. J. Immunol. **174**, 3501–3507.
16. Leishman, A. J., Naidenko, O. V., Attinger, A., Koning, F., Lena, C. J., Xiong, Y. et al. (2001). T cell responses modulated through interaction between CD8αα and the nonclassical MHC class I molecule, TL. Science, **294**, 1936–1939.
17. Campbell, N. A., Park, M. S., Toy, L. S., Yio, X. Y., Devine, L., Kavathas, P. & Mayer, L. (2002). A non-class I MHC intestinal epithelial surface glycoprotein, gp180, binds to CD8. Clin. Immunol. **102**, 267–274.
18. Kern, P. S., Teng, M. K., Smolyar, A., Liu, J. H., Liu, J., Hussey, R. E. et al. (1998). Structural basis of CD8 coreceptor function revealed by crystallographic analysis of a murine CD8αα ectodomain fragment in complex with H-2K^b. Immunity, **9**, 519–530.
19. Liu, Y., Xiong, Y., Naidenko, O. V., Liu, J. H., Zhang, R., Joachimiak, A. et al. (2003). The crystal structure of a TL/CD8αα complex at 2.1 Å resolution: implications for modulation of T cell activation and memory. Immunity, **18**, 205–215.
20. Laskowski, R. A., MacArthur, M. W., Moss, D. S. & Thornton, J. M. (1993). PROCHECK: a program to

check the stereochemical quality of protein structures. J. Appl. Crystallog. **26**, 283–290.
21. Wilson, I. A. & Stanfield, R. L. (1994). Antibody-antigen interactions: new structures and new conformational changes. Curr. Opin. Struct. Biol. **4**, 857–867.
22. Devine, L., Rogozinski, L., Naidenko, O. V., Cheroutre, H. & Kavathas, P. B. (2002). The complementarity-determining region-like loops of CD8α interact differently with β2-microglobulin of the class I molecules H-2K^b and thymic leukemia antigen, while similarly with their α3 domains. J. Immunol. **168**, 3881–3886.
23. Qin, S. X., Wise, M., Cobbold, S. P., Leong, L., Kong, Y. C., Parnes, J. R. & Waldmann, H. (1990). Induction of tolerance in peripheral T cells with monoclonal antibodies. Eur. J. Immunol. **20**, 2737–2745.
24. Marshall, S. E., Cobbold, S. P., Davies, J. D., Martin, G. M., Phillips, J. M. & Waldmann, H. (1996). Tolerance and suppression in a primed immune system. Transplantation. **62**, 1614–1621.
25. Parish, N. M., Bowie, L., Zusman Harach, S., Phillips, J. M. & Cooke, A. (1998). Thymus-dependent monoclonal antibody-induced protection from transferred diabetes. Eur. J. Immunol. **28**, 4362–4373.
26. Devine, L., Sun, J., Barr, M. R. & Kavathas, P. B. (1999). Orientation of the Ig domains of CD8αβ relative to MHC class I. J. Immunol. **162**, 846–851.
27. Zajonc, D. M., Elsliger, M. A., Teyton, L. & Wilson, I. A. (2003). Crystal structure of CD1a in complex with a sulfatide self antigen at a resolution of 2.15 Å. Nature Immunol. **4**, 808–815.
28. Altmann, F., Staudacher, E., Wilson, I. B. & Marz, L. (1999). Insect cells as hosts for the expression of recombinant glycoproteins. Glycoconj. J. **16**, 109–123.
29. Kantardjieff, K. A. & Rupp, B. (2003). Matthews coefficient probabilities: improved estimates for unit cell contents of proteins, DNA, and protein-nucleic acid complex crystals. Protein Sci. **12**, 1865–1871.
30. Navaza, J. (1994). AMoRe: an automated package for molecular replacement. Acta Crystallog. sect. A, **50**, 157–163.
31. Ghiara, J. B., Stura, E. A., Stanfield, R. L., Profy, A. T. & Wilson, I. A. (1994). Crystal structure of the principal neutralization site of HIV-1. Science, **264**, 82–85.
32. Brünger, A. T., Adams, P. D., Clore, G. M., DeLano, W. L., Gros, P., Grosse-Kunstleve, R. W. et al. (1998). Crystallography & NMR system: a new software suite for macromolecular structure determination. Acta Crystallog. sect. D, **54**, 905–921.
33. Murshudov, G. N., Vagin, A. A., Lebedev, A., Wilson, K. S. & Dodson, E. J. (1999). Efficient anisotropic refinement of macromolecular structures using FFT. Acta Crystallog. sect. D, **55**, 247–255.
34. Collaborative Computational Project, Number 4. (1994). The CCP4 suite: programs for protein crystallography. Acta Crystallog. sect. D, **50**, 760–763.
35. Jones, T. A., Zou, J.-Y., Cowan, S. W. & Kjeldgaard, M. (1991). Improved methods for building protein models in electron density maps and the location of errors in these models. Acta Crystallog. sect. A, **47**, 110–119.
36. Connolly, M. L. (1993). The molecular surface package. J. Mol. Graph. **11**, 139–141.
37. Kraulis, P. J. (1991). MOLSCRIPT: a program to produce both detailed and schematic plots of protein structures. J. Appl. Crystallog. **24**, 946–950.

Edited by R. Huber

(Received 9 December 2005; received in revised form 2 February 2006; accepted 8 February 2006)
Available online 23 February 2006